Magnetic field enhanced detection of coherent phonons in a GaMnAs/GaAs film

Brenden A. Magill,[1] Sunil Thapa,[2] Jade Holleman,[3] Stephen McGill,[3] Hiro Munekata,[4] Christopher J. Stanton,[2,*] and Giti A. Khodaparast[1,†]

[1]*Department of Physics, Virginia Tech, Blacksburg, Virginia 24061, USA*
[2]*Department of Physics, University of Florida, Gainesville, Florida 32611, USA*
[3]*National High Magnetic Field Laboratory, Tallahassee, Florida 32310, USA*
[4]*Laboratory for Future Interdisciplinary Research of Science and Technology (FIRST), Tokyo Institute of Technology, 4259-R2-57 Nagatsuta, Midori-ku, Yokohama 226-8503, Japan*

(Received 14 December 2019; revised 5 May 2020; accepted 16 June 2020; published 20 July 2020)

Using a two-color time-resolved pump-probe spectroscopy scheme, we studied the generation and detection of longitudinal coherent acoustic phonons, generated by ultrafast laser pulses in a semiconductor heterostructure. Our structure was a *p*-doped, 100-nm-thick ferromagnetic GaMnAs layer grown on a GaAs substrate. By probing the transient reflectivity in the time domain, we observed *a strong dependence* of the coherent phonon's amplitude on the external magnetic field. Our theoretical model relates this dependence to the increase in the *detectability* of coherent phonons in the presence of external magnetic fields. This enhancement comes from the formation of Landau levels in the absorption spectrum and leads to large changes in the real and imaginary parts of the dielectric function with strain. When the probe laser energy is close to an allowed Landau-level transition, the detectability of the coherent phonons can be significantly enhanced. Our results suggest that not only can one increase the detection of coherent phonons with magnetic fields, one can also enhance the *generation* by tuning the wavelength of the pump laser pulse to coincide with a Landau-level resonance.

DOI: 10.1103/PhysRevB.102.045306

I. INTRODUCTION

Time-resolved (TR) spectroscopy in semiconductors is a powerful tool for probing the relaxation dynamics of photoexcited carriers [1–8]. After photoexcitation, the nonequilibrium electrons relax by several scattering mechanisms such as carrier-carrier, carrier-phonon, and carrier-impurity scattering [9,10]. In addition to creating nonequilibrium electron-hole pairs, the ultrafast optical excitation of a semiconductor can generate *coherent phonons* (CPs), which, depending on the excitation conditions, can be either optical or acoustic and are detected as oscillations in the differential transmission or reflection [11].

The ability to control these CPs and hence the vibrational, thermal, and phononic properties of semiconductor nanostructures has important technological impacts. Possible applications include heat management [12,13], charge transfer [14], and phonon lasing [15–18]. Methods of tailoring and controlling vibrational properties in the past have relied on interdigitated transducers to generate surface acoustic waves in a variety of applications [19]. By tailoring materials and excitation conditions, one can control the photogenerated optical CPs [9,10] as well acoustic CP wave packets (nonequilibrium strain pulses) which propagate into a semiconductor and trigger oscillations in the optical properties by modulating the position-dependent dielectric function [11,20–25]. Such techniques can be used to control electric, magnetic, and strain fields and lead to revolutionary new devices.

In several coherent dynamics measurements, in weak excitation regimes, nonthermal excitations were considered to be the dominating mechanism [1,2,6,26–29]. In the strong excitation regime, ultrafast demagnetization has been attributed to thermal [30–32] aspects of the excitation. However, in ferromagnetic structures, CPs at high magnetic fields have not been explored extensively.

II. EXPERIMENTAL APPROACH

In this work we investigated the *magnetic field dependence* of the CPs in a ferromagnetic GaMnAs film grown on GaAs, for B fields ranging from 0 to 10 T, and we used 400-nm pump and 800-nm probe pulses with ∼100-fs pulse width and 1-kHz repetition rate. Compared to the study by Qi *et al.* [4], our structure has a larger Mn content and is a thinner molecular-beam-epitaxy–grown film consisting of a 100-nm $Ga_{1-x}Mn_xAs$ ($x = 0.082$) layer on top of a GaAs substrate. We also used 800-nm probe pulses tuned above the low-temperature band gap of GaAs. Our structure has a T_c of 110 K, and the growth details have been reported earlier [1]. Our experimental results show a *strong dependence* of the CP's oscillation on magnetic field and agree with a theoretical model which predicts this enhancement.

In an earlier study by Qi *et al.* [4], CP dynamics were probed in 1-μm-thick $Ga_{1-x}Mn_xAs$ films on GaAs substrates with different Mn contents ($x = 0.03$, 0.05, and 0.07). In their study, the structures had Curie temperatures (T_c) below 53 K,

*Corresponding author: stanton@phys.ufl.edu
†Corresponding author: khoda@vt.edu

and to generate and probe CPs, 400-nm pump and 830-nm probe pulses (below the gap in GaAs at low temperature) at $B = 0$ were employed. They observed a change in the CP velocity in the GaMnAs layer originating from a change in the elastic constant.

Our observations presented in this study indicate that at least some of the acoustic CPs that are generated by the 400-nm pump pulse come from the *interface* between the ferromagnetic GaMnAs layer and the GaAs substrate. We believe this results from the strong built-in electric fields near the highly *p*-doped GaMnAs and undoped GaAs, which can rapidly trap photoexcited charge carriers at the interface and trigger coherent phonons from the interface. Furthermore, by employing an external magnetic field we were able to demonstrate the enhancement and tunability of the magnitude of the CPs [33]. Our observed strong magnetic field dependence of the CP dynamics can open new directions to study ferromagnetic semiconductors [3,34–37] and other multifunctional materials such as the ones in our earlier study of barium titanate-bismuth ferrite films and nanorods [38]. Our result and model provide a new direction to employ CPs in sensing and devices with a capability to dynamically control the (i) amplitude, (ii) frequency, and (iii) phase of the coherent oscillations and strain pulses. The variation of these three quantities are discussed in the Appendix, where we present the experimental observations and compare them with our model.

The two-color pump-probe configuration in this work is similar to the studies reported in Mudiyanselage *et al.* [38]. The pump and probe wavelengths were 400 and 800 nm, respectively. Our laser spot size was ∼150 μm in diameter. Prior to employing our pump-probe measurements, the sample was cooled to 5 K in the absence of an external magnetic field and maintained at the same temperature during the entire measurement process. The sample was mounted with the field direction slightly off [010] towards [-110]. The 400-nm pump pulse has a short absorption length, about 15 nm, while the 800-nm probe pulse has a long absorption length (about 0.74 μm) and hence can penetrate deeply into the sample. Thus, the dynamics of the CP generation are driven by the interaction between the pump pulse and the GaMnAs layer and/or interface with the substrate, while the detection is sensitive to changes both in the GaMnAs and GaAs substrate layers.

Figure 1 presents our time-resolved differential reflectivity (TRDR) measurements by increasing the magnetic field from 0 to 10 T. These oscillations displayed periods between 23.3 and 24.6 ps. This corresponds to a period much shorter than the reported periods for magnetic procession in GaMnAs [3]. We note, however, that our observed period of oscillations is in the correct range for coherent longitudinal acoustic (LA) phonons [4,39]. As shown in Fig. 1, the amplitude of the CP oscillations changes *substantially* and shows a significant increase as a function of external magnetic field compared to the $B = 0$. In the inset of Fig. 1, we present traces for 8 and 10 Tesla, where the initial rise due to carrier dynamics was removed. In the inset we compare the evolution of the amplitude and phase of the CPs at 8 and 10 T. While there is an overall increase in the amplitude with changing the magnetic field in Fig. 1, one can easily see that it is not monotonic.

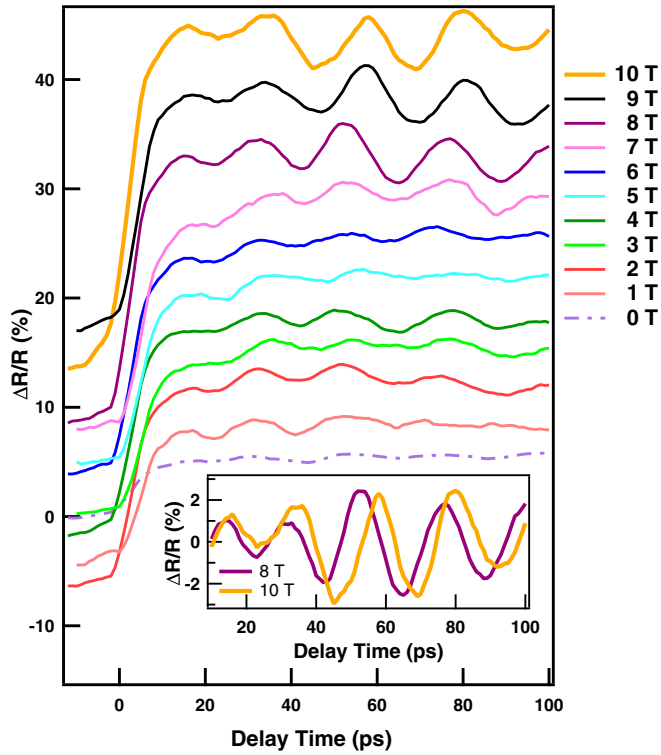

FIG. 1. Experimental time-resolved differential reflectivity for a two-color 400-nm pump/800-nm probe scheme with an average pump power of 1.6 mW at 5 K in an external magnetic field from 0 to 10 T (legend on right) with traces offset so that the evolution of the oscillations can be observed as a function of increasing the magnetic field. The inset shows an example of the oscillations at 8 T and 10 T, with the initial carrier dynamics excluded. Note the change in phase between the two traces.

III. THEORETICAL MODEL

The change in the differential reflectivity $\Delta R/R$ is related to the changes in the index of refraction. For a uniform system, with small pump-induced changes to the reflectivity, it is given by

$$\Delta R/R = 2\mathrm{Re}\left\{\int_0^\infty e^{i2kx}\frac{\delta}{\delta x}\delta n(x,t)dx\right\}, \tag{1}$$

where n is the complex index of refraction, δn is the change in the complex index of refraction which is position dependent and originates from the propagating strain induced by the pump pulse, and $k = nk_0$.

For GaAs at 800 nm (and also GaMnAs), the imaginary part of the index of refraction is much smaller than the real part, and as a result, we can take the index n to be real. Note, however, that for the change in the index of refraction δn due to the pump pulses, both the real and imaginary parts can be important. The change in the index of refraction δn induced by the pump pulse can be related to the change in the dielectric constant ε, which in turn can be related to the propagating strain η and the deformation potential a_{cv}:

$$2n\delta n = \delta\varepsilon = -a_{cv}\frac{\partial\varepsilon}{\partial E_g}\eta. \tag{2}$$

The picture we present here relates a rigid shift in the energy gap E_g due to the strain where the magnitude of the energy shift is determined by the deformation potential. Typically, as the strain wave propagates into the sample, it leads to a localized change in the index of refraction, whose position changes with time. This leads to an additional reflection of the probe pulse off of this localized change in the index, which can interfere with the reflection off the surface (known as Brillouin oscillations). As the strain pulse propagates into the sample, the interference alternates between constructive and destructive, and this leads to oscillations in $\Delta R/R$.

In the linear regime, the strain pulse propagates undistorted through the media with a velocity v_s, and it can be shown (at long times) that $\Delta R/R$ is given by [40,41]

$$\frac{\Delta R}{R} \propto 2\mathrm{Re}\left\{\frac{\partial \varepsilon}{\partial E}\ e^{i2kv_s t}\int_{-\infty}^{\infty} e^{i2ku}\frac{\delta}{\delta u}\delta\eta_0(u)du\right\}, \quad (3)$$

with η_0 the initial strain profile. We can notice from the exponential term in Eq. (3) that $\Delta R/R$ will oscillate with a period T given by $T = \lambda_0/(2nv_s)$. For probe wavelengths where the imaginary part of the index is large, the reflectivity signal will be damped out as the strain pulse goes into the sample.

The amplitude of the oscillations will be affected by $\frac{\partial \varepsilon}{\partial E}$, the derivative of the real and imaginary part of the complex dielectric function with respect to energy [42], which are similar to the Seraphin coefficients [43]. We can write this derivative as

$$\frac{\partial \epsilon}{\partial E} = \sqrt{\left(\frac{\partial \epsilon_r}{\partial E}\right)^2 + \left(\frac{\partial \epsilon_i}{\partial E}\right)^2}\ e^{i\phi_\epsilon}. \quad (4)$$

Thus the amplitude of $\Delta R/R$ is directly related to the magnitude of this derivative of the complex dielectric function.

Without the presence of magnetic field, the absorption coefficient (above the band gap) is relatively slowly varying with energy. A strain pulse modulating the dielectric function thus only has a small effect on the change in reflectivity. In contrast, in the presence of a magnetic field, the absorption becomes strongly peaked with the electronic states becoming Landau levels. If one is probing near one of these Landau-level resonances, then the strain pulse leads to a large change in the dielectric function near this resonance, which leads to a large change in the differential reflectivity.

To understand how the amplitude in Eq. (4) depends on external magnetic field, we will use a simple model based on a harmonic oscillator. In a two-dimensional system using a two-band semiconducting model in a magnetic field, the energy levels of the free-electron gas can be represented as Landau levels. The absorption spectra (related to the imaginary part of the dielectric function) now becomes a series of discrete, harmonic oscillator resonant transitions (which are broadened) with the energy levels given by

$$\hbar\omega_n = E_g + \left(n + \frac{1}{2}\right)eB\left(\frac{1}{m_e^*} + \frac{1}{m_h^*}\right), \quad (5)$$

where m_e^* and m_h^* are the effective mass of the electron and hole bands, respectively. In three dimensions, in a more realistic semiconductor like GaAs, one must take into account many more effects: (1) There is still a k_z quantum number which leads to a $1/\sqrt{E}$ density of states, in addition to the discrete Landau levels. (2) There are multiple valence bands (heavy-hole, light-hole, and spin-split hole bands.) (3) The bands deviate from simple parabolic bands. (4) Exciton effects should be taken into account. Nonetheless, the absorption spectra (see Fig. 2) can be seen to be approximated by a series of peaks originating from the Landau-level transitions. In three dimensions, we can still approximate the Landau levels as a series of harmonic oscillator transitions that are further broadened (owing to the one-dimensional density of states coming from the k_z quantum number).

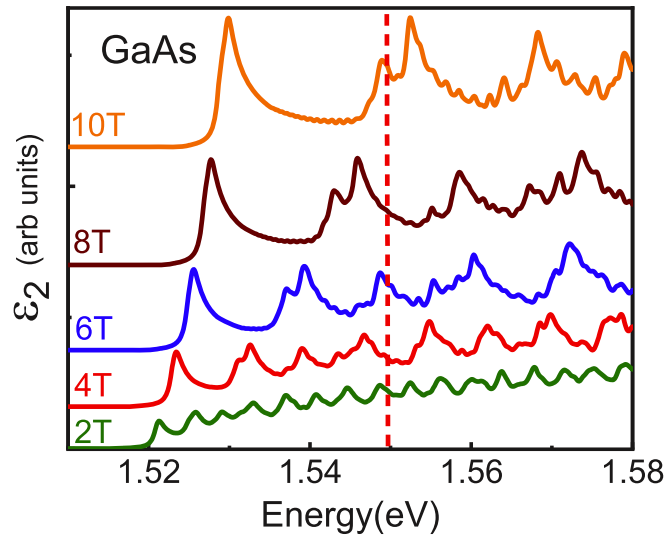

FIG. 2. The calculated imaginary part of the dielectric function ϵ_2 for GaAs as a function of photon energy from $B = 2$–10 Tesla. The traces are offset for clarity. The dashed line in the graph denotes the energy of the photons in the probe pulse (1.55 eV). Excitonic effects are not included.

In Fig. 2 we plot the calculated imaginary part of the dielectric function ϵ_2 as a function of energy for magnetic fields ranging from 2 to 10 T for bulk GaAs. Calculations have been performed with an eight-band $k \cdot P$ method that does not include many-body interactions that we have discussed previously [44,45]. We observe that the effect of increasing the magnetic field is to increase the strength of the absorption in a given Landau-level transition as well as their separation. As the magnetic field increases, the density of states (for $B = 0$) mapped into a given Landau level increases, resulting in an increase in strength as well as an increase in spacing between the Landau levels. In Fig. 2, a dotted line shows the energy of the probe pulse (800-nm wavelength, 1.55-eV energy).

To model the effect of a single Landau level, we use a simple harmonic oscillator model and consider the effect of one oscillator with frequency ω_o on the dielectric function. One can write the dielectric function in terms of the susceptibility χ by $\varepsilon = \varepsilon_0(1 + \chi)$. The magnitude of the $\Delta R/R$ oscillations is then determined by the derivative of the real and imaginary parts of χ with respect to energy. The susceptibility for a

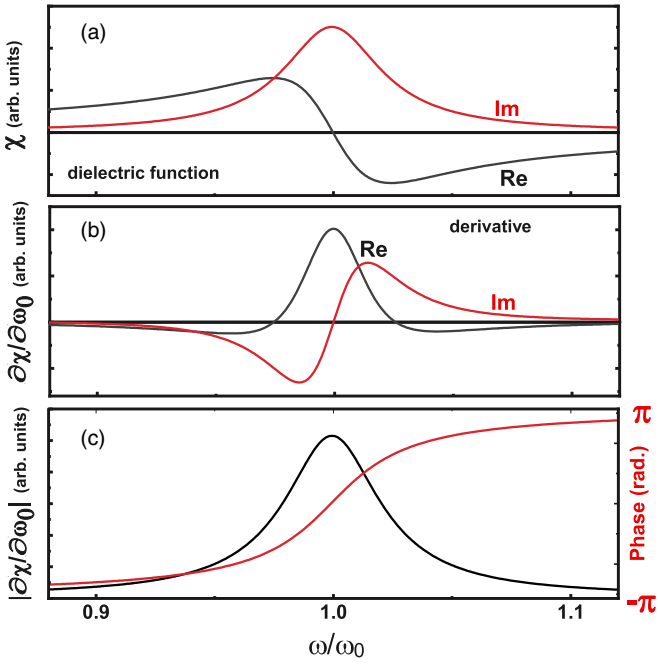

FIG. 3. (a) The real and the imaginary components of the susceptibility $\chi(\omega) = \chi' + i\chi''$ for our oscillator model. (b) The real and the imaginary parts of the derivative of the χ with respect to ω_0. (c) The amplitude and the phase of the derivative. The phase ϕ is given by $\tan\phi = \frac{d\chi''/d\omega_0}{d\chi'/d\omega_0}$.

harmonic oscillator is well known and is given by

$$\chi = \frac{\omega_p^2}{\omega_0^2 - \omega^2 - i\frac{\omega}{\tau}}. \tag{6}$$

When the CP strain pulse propagates through the sample, it will change the band gap E_g and hence the frequency of the resonant transition ω_0, according to Eq. (5). The derivative of this susceptibility with respect to the resonant frequency ω_0 is given by

$$\frac{\partial\chi}{\partial\omega_0} = \frac{-2\omega_0\omega_p^2}{\left(\left(\omega_0^2 - \omega^2\right)^2 + \left(\frac{\omega}{\tau}\right)^2\right)^2}\left\{\left[\left(\omega_0^2 - \omega^2\right)^2 - \left(\frac{\omega}{\tau}\right)^2\right] + 2i\left(\omega_0^2 - \omega^2\right)\frac{\omega}{\tau}\right\}. \tag{7}$$

The real and imaginary parts of χ and its derivative are plotted in Figs. 3(a) and 3(b), and the magnitude and phase of the derivative are plotted in (c). We now have an insight into the increase of the strength of the CP oscillations with magnetic field. When a magnetic field is applied, the susceptibility becomes a series of peaks resulting from the Landau-level formation, and both the strength and the separation of the peaks will increase with applying magnetic fields.

Therefore if one is probing with a wavelength near one of the peaks, then the amplitude of the oscillations will increase significantly, since the signal is proportional to the *derivative,* which is also strongly peaked near the transition. This fact enhances the *detectability* of the CPs. While the strength of the peaks increases linearly with magnetic field, the actual increase in the CP signal depends explicitly on where the probe energy is with respect to the Landau-level transitions. As a result, the amplitude may not increase monotonically with the magnetic field.

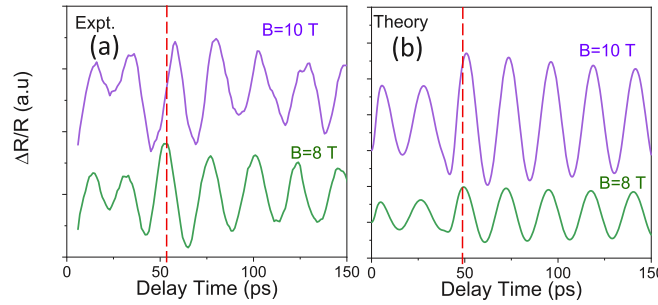

FIG. 4. (a) TRDR for 8 and 10 Tesla at 5 K. To focus on the oscillations, the initial carrier dynamics have been subtracted out. Our theoretical predictions for the CP oscillations are shown in (b). The red dashed line marks a point in time when the strain pulse (generated at the *interface* between the GaMnAs layer and GaAs substrate) reflects off the surface and returns to the interface between the GaMnAs and the GaAs and is in the GaAs substrate. A change in the phase of the oscillation can be seen between the 8- and 10-T traces, for both theory and experiment.

We also looked into the variation of the dielectric function in GaMnAs. In the 800-nm range of the probe, the absorption in GaMnAs is very weak and flat. This results from the fact that the GaMnAs is heavily p doped. As a result, the Fermi level lies deep within the valence bands and there are no valence-band–to–conduction-band Landau-level transitions. Instead, there are some inter-valence-band transitions that can give rise to some absorption. These transitions do not have the sharp-peaked Landau-level structure that the valence-to-conduction-band transitions have. As a result, the derivatives of the real and imaginary parts of the dielectric function in GaMnAs are much smaller, indicating that the oscillations that we observe are dominated by the acoustic modes propagating in the GaAs substrate.

In Fig. 2 the fixed energy of the probe laser pulse is marked with a red dashed line. As the field increases, one observes that the probe is not always at the peak of the Landau level and in fact can be either at the peak or on either side of the level or in between Landau levels. As a result, the enhancement of the CP signal does not increase monotonically with magnetic field. While the strength of the Landau levels increases with magnetic field, the CP signal can actually go down with B if one is probing between the Landau levels for that field. This has been seen experimentally in Fig. 1, where we see the amplitude drop at 5 T. In addition, depending on what side of the Landau level the probe pulse lies, the phase of the CP oscillations can also change, as can be seen in Fig. 3(c). This has been observed experimentally in changing the field from 8 to 10 T, where a strong phase change is seen and is shown in Fig. 4. The theoretically calculated phase change is not as strong, and this will be discussed further in the Appendix when we consider the role of broadening of the transitions. In addition, we note that excitonic effects are not included in our model. The inclusion of excitonic effects will quantitatively modify the enhancement factor and can also alter the phase

change by changing the position and shape of the Landau levels.

We also note that for the first ∼45 ps, the amplitude of the CP is smaller than after 45 ps (both experimentally and theoretically). This delay time (45 ps) is *twice* the time it takes for the strain pulse to go from the surface to the interface. This indicates to us that part of the strain pulse is generated near the GaMnAs/GaAs interface. We believe that this results from the strong built-in electric fields between the heavily *p*-doped GaMnAs and the undoped GaAs, which can rapidly trap carriers near the interface and trigger a strain pulse which originates from the interface [46]. The longitudinal speed of sound in the [100] direction in GaAs is about 4.73 nm/ps (which is slightly higher than in GaMnAs). The transit time t_{trans} is the time that would take a longitudinal strain pulse to go from the surface to the interface (100 nm away), and it would be 21.14 ps. The change in oscillation amplitude as shown in the inset of Fig. 1 is twice that of $t_{\text{trans}} = 42.28$ ps.

How then do we get a strain pulse generated at the interface? We believe that the initial, nonequilibrium, exponentially decaying photoexcited carrier distribution evolves through diffusion. In fact, previous studies [47] which investigated the coupling between coherent optic phonons and plasmons in a 400-nm pump/800-nm probe scheme in GaAs showed a rapid change in the coupled plasmon-phonon modes on a picosecond or subpicosecond timescale. This rapid change was attributed to diffusion of photoexcited carriers away from the surface. Based on these earlier studies, our best estimate for the diffusion constant is 30 cm^2/s.

At the interface, strong built-in electric fields (due to the difference in doping in the GaMnAs layer, which is very highly *p* doped, and the GaAs substrate, which is not intentionally doped) can trap the carriers at the interface. Hence, within 1 ps of the pump pulse, a large number of carriers can be trapped at the interface and generate a strain pulse that propagates in both directions from the interface. This indicates to us that a strain pulse is generated at the interface (which is the stronger pulse) and can propagate in both directions (into the GaAs sample as well as into the GaMnAs film). The time it takes for the pulse at the interface to reflect off the surface and return to the interface is 42.28 ps since it has to transit the 100-nm GaMnAs film twice. A similar effect has been observed in interfaces between GaAs and transition-metal oxides with large interfacial electric fields [48].

IV. CONCLUSION

In conclusion, we studied the ultrafast generation of coherent longitudinal acoustic phonons in a system consisting of a ferromagnetic GaMnAs thin film grown on a GaAs substrate as a function of applied magnetic field. We found an extremely large enhancement in the amplitude of the Brillouin oscillations with an increase in magnetic field. This enhancement occurs primarily in the GaAs layer and results from a change in the dielectric function due to the formation of Landau levels, which enhances the *detectability* of the phonons. The differential reflectivity is proportional to the derivative of the dielectric function, which is strongly peaked near a Landau-level transition. As the magnetic field increases, the strength of the Landau-level transitions also increases. This fact leads to a general overall increase in the CP's oscillation amplitudes with increasing magnetic field, provided the probe energy is near the peak of a Landau level. The increase with field, however, is not monotonic, since the probe energy can lie between Landau levels where the enhancement effect is weaker.

Although the details depend on the exact position where the probe energy is with respect to the Landau levels, the CPs when propagating inside the GaMnAs layer did not show a strong increase in the amplitude of the oscillations with magnetic field. This is because the GaMnAs layer is highly doped, and as a result, the lowest valence-band–to–conduction-band Landau levels at the probe wavelength are blocked (Burstein-Moss effect), leading to a small derivative in the dielectric function at the probe wavelength for GaMnAs and hence a small response from the GaMnAs layer.

While our studies demonstrated an external magnetic field can lead to a large enhancement in the *detection* of the CPs, perhaps a more interesting application would be to use the magnetic field to enhance the *generation* of the CPs. This could be accomplished by tuning the Landau levels into and out of resonance with the *pump pulses.* Our study has shown that the amplitude, frequency, and phase of the CP oscillations can be extremely sensitive to the external magnetic fields and suggests that CPs can be used for probing the quantum states of multilayer materials.

ACKNOWLEDGMENTS

This material is based upon work supported by the Air Force Office of Scientific Research under Awards No. FA9550-14-1-0376, No. FA9550-17-1-0341, and No. FA9550-16-1-0358 under the DURIP2016 program. A portion of this work was performed at the National High Magnetic Field Laboratory, which is supported by the National Science Foundation through Cooperative Agreements No. DMR-1157490 and No. DMR-1644779 and the State of Florida. We acknowledge technical supports from Dr. N. Nishizawa and S. Ogawa members of Munekata-lab at Tokyo Institute of Technology (TIT). This work was supported in part by the TIT Research Abroad and Invitational Program for International Collaboration, and Grant-in-Aid for Scientific Research No. 22226002 and No. 18H03878.

B.A.M. and S.T. contributed equally to this work.

APPENDIX: MAGNETIC-FIELD DEPENDENCE IN DETAIL

In this Appendix we provide more details on the magnetic field dependence of the real and imaginary parts of the dielectric function, as well as the enhancement in amplitude. Figure 5(a) shows the variation of $\epsilon_i(E)$ as a function of external magnetic field. For the undoped GaAs, the interband Landau-level resonance energy gets shifted to higher energies and increases in strength by increasing the magnetic field. Consequently, a significantly different value of the dielectric function corresponds to the probe energy of 1.55 eV, and by

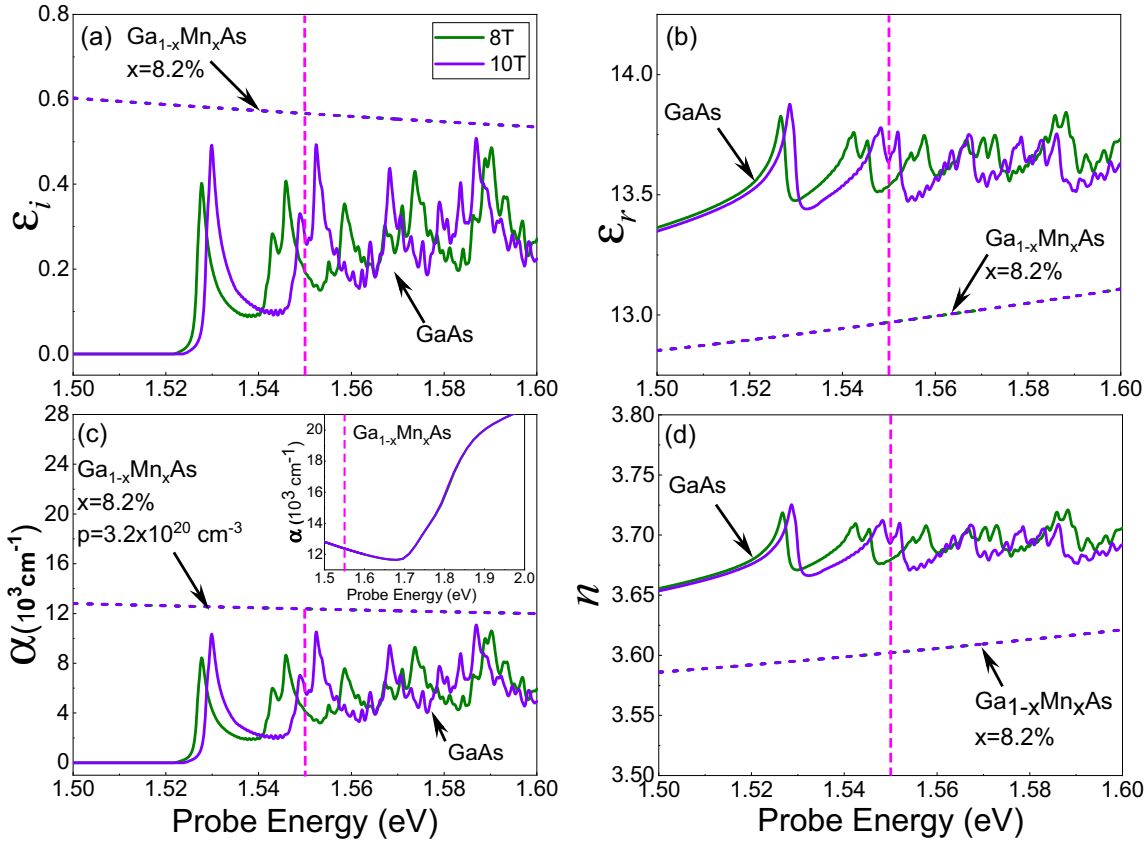

FIG. 5. Magnetic field dependence of the imaginary (a) and the real (b) part of the dielectric function as well as (c) the absorption coefficient and (d) the refractive index for GaMnAs (dashed lines) and GaAs (solid lines) calculated at $B = 8$ and 10 T. Inset in (c) shows the interband absorption for the GaMnAs in a wider scale.

the Kramer's-Kronig relations, $\epsilon_r(E)$ changes accordingly, as seen in Fig. 5(b). The corresponding dependence on magnetic field of the absorption coefficient $\alpha(E)$ and the real refractive index $n(E)$ are shown in Figs. 5(c) and 5(d). The inset in Fig. 5(c) shows the magneto-absorption for GaMnAs in a wider scale.

However, in the highly p-doped GaMnAs, the interband resonances from the highest valence bands to the lowest

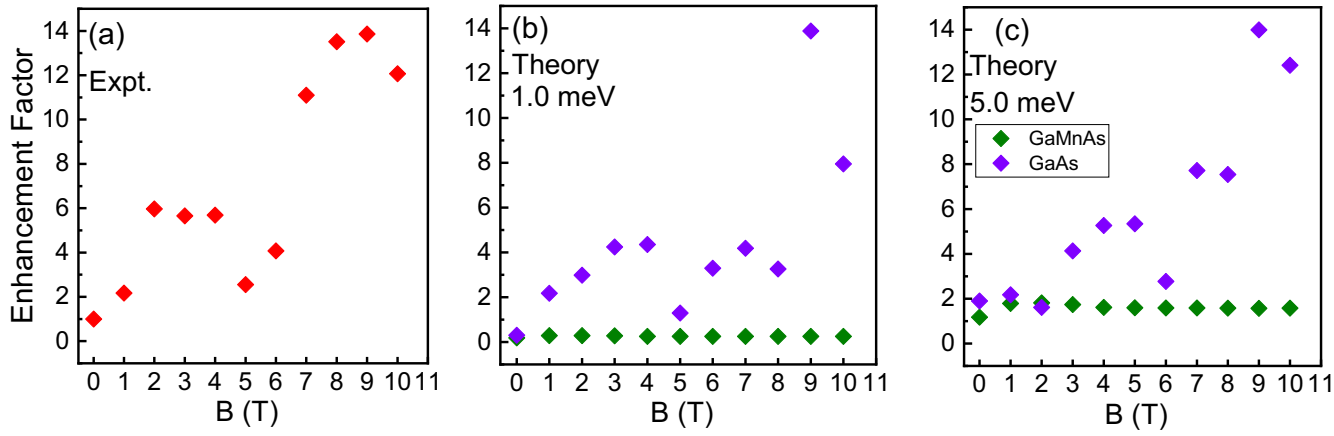

FIG. 6. The enhancement factor of the amplitude of the CP oscillations as a function of magnetic field for (a) the experimental observation, (b) theoretical calculations with a broadening of 1 meV in the GaAs layer, and (c) theoretical calculations with a broadening of 5 meV in the GaAs layer. The theoretical calculations show both the enhancement factor for GaAs (violet diamonds) and GaMnAs (green diamonds) and are normalized to the experimental value at $B = 1$ T. The GaMnAs layer has a much higher Landau-level broadening due to the very high p doping in that layer.

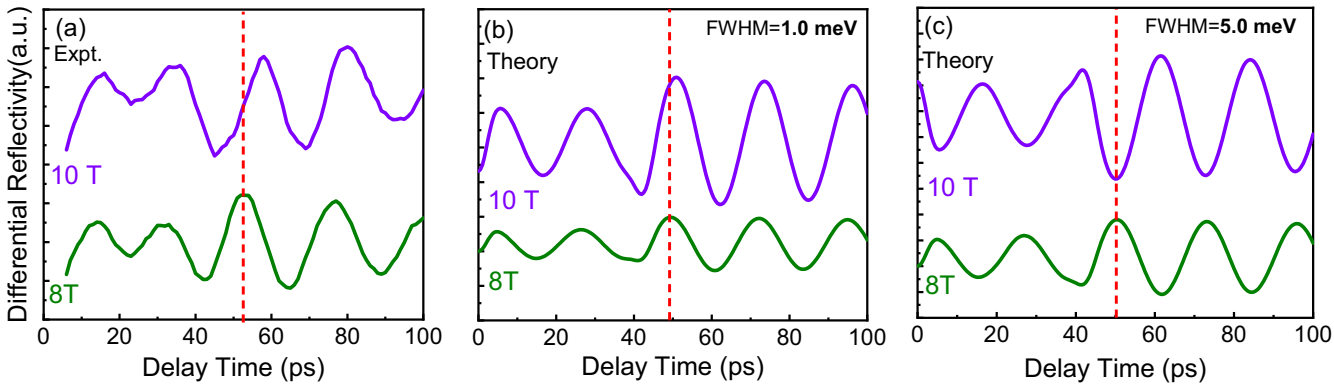

FIG. 7. Comparison of the CP oscillation's phase at 50 ps by varying the field from 8 and 10 T for (a) the experimental data, (b) the theoretical model with 1-meV broadening, and (c) the theoretical model with 5-meV broadening. As can be observed by comparing the figures, the peak of the 10-T oscillation in (b) with 1-meV broadening lags behind the peak of the 8-T oscillation by a small amount, somewhat less than the experimentally observed response. For (c) with 5-meV broadening, the peak at 10 T lags the peak at 8 T more than the experimental data. These results suggest that the actual broadening may lie between 1 and 5 meV. This will depend, of course, on the exact position of the peak in the Landau level.

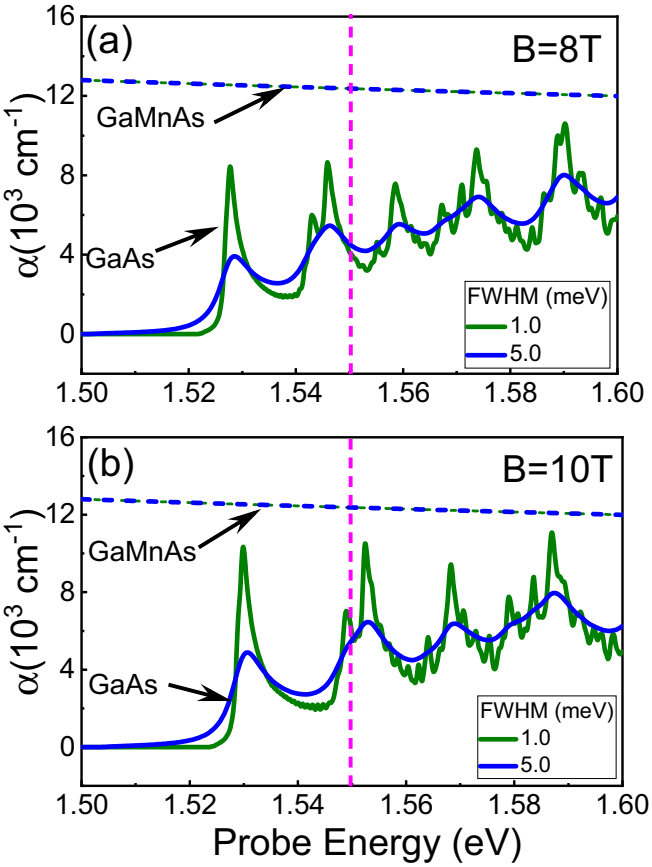

FIG. 8. Absorption spectra for GaAs and GaMnAs for $B = 8\,\mathrm{T}$ (a) and $B = 10\,\mathrm{T}$ (b) with 1-meV broadening (green) and 5-meV broadening (blue). For $B = 8\,\mathrm{T}$ (a), the probe energy is on the same side of the absorption feature, hence the phase does not change much with the broadening in Fig. 7. For $B = 10\,\mathrm{T}$ (b), for small broadening (1 meV), the probe is located on the right-hand side of a light-hole Landau-level transition and hence the phase difference between 8 and 10 T is not that large. For larger broadening (5 meV), the light- and heavy-hole transitions are combined into one broad transition. Now the probe is on the left-hand side of this transition leading to an almost π phase change between 8 and 10 T. (See Fig. 3 in the main text.)

conduction band are absent at the probe energy due to high doping which leads to a Burstein-Moss shift, as evidenced in Fig. 5(c) (and also the inset). Moreover, the high doping in the GaMnAs layer leads to large broadening of the transitions, since the mobility in the GaMnAs layer is much lower than the undoped GaAs substrate. Hence, the inter-valence-band absorption spectrum in GaMnAs remains essentially flat, suggesting no significant change in the dielectric function and the optical constants by varying the magnetic field.

In Fig. 6(a) we present the experimental enhancement factors of the CP's amplitude as a function of magnetic field and compare them with our theoretical model for two different Landau-level broadenings in the GaAs layer; Fig. 6(b) is for 1 meV and Fig. 6(c) presents the result for 5 meV. Because of the high p doping in the GaMnAs layer, the transitions have even larger broadening. The theoretical results show the following: (i) the change in enhancement is dominated by the GaAs layer for $B \neq 0$ for 1-meV broadening and for $B \geqslant 3T$ for 5-meV broadening; (ii) there is an increase in enhancement factor as one goes to higher magnetic fields, which is associated with the increase in density of states of the Landau levels with magnetic field; (iii) the increase is not monotonic, since the probe energy can be between Landau levels for certain values of magnetic field (like in the 5-T region seen here); and (iv) the enhancement factor depends strongly on the exact position and broadening of the Landau levels. In Fig. 6(c) we show that a 5-meV broadening can more accurately reproduce the experimental results than a 1-meV broadening presented in Fig. 6(b). For 5-meV broadening, the GaMnAs enhancement factor is comparable to the GaAs factor for $B \leqslant 2$, which might explain a slightly different period for the shortest times that is experimentally observed (cf. Fig. 9).

In Fig. 7 we present the sensitivity of the CP's oscillation phase to the applied magnetic fields at the time (50 ps). (This is when the strain pulse which originated at the interface has reflected off the surface and is back in the GaAs layer.) We compared this observation with our model for two different Landau-level broadenings (1 and 5 meV). We can observe

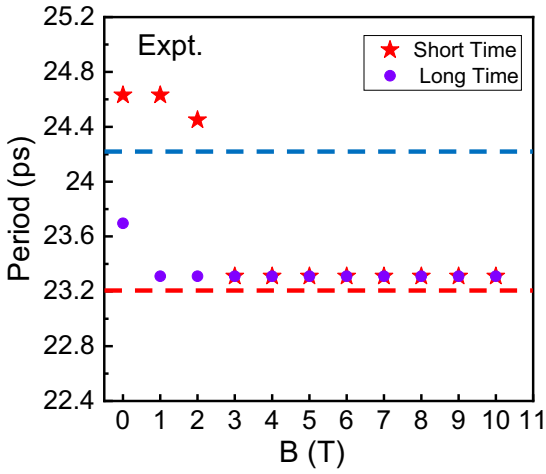

FIG. 9. Experimentally measured period of the CP's oscillations at the initial propagation times < 40 ps (red star) and longer times >50 ps (violet circle) as a function of magnetic field. The red dashed line is a theoretical calculation, and the blue line is an estimate for the $Ga_{1-x}Mn_xAs$ with $x = 0.07$.

for 1-meV broadening, in Fig. 7(b), that the calculated phase at 10 T slightly lags behind the 8-T result. The phase lag is less than the experimental one, shown in Fig. 7(a). In comparison, for 5-meV broadening in Fig. 7(c), the 10-T phase significantly lags the 8-T phase. To understand this, we have plotted the absorption spectra for $B = 8$ T in Fig. 8(a) and $B = 10$ T in 8(b), for both 1- and 5-meV broadening. The dashed red line corresponds to the probe energy. We observe that for 8 T, for either 1- or 5-meV broadening, the probe is on the right-hand side of the absorption feature, and as a result, the phase for 8 T does not change much with broadening.

In contrast, for 10 T and 1-meV broadening, the probe is on the right-hand side of a light-hole Landau-level transition, and as a result, only has a small phase difference compared to the 8-T oscillation. For 5-meV broadening, the light-hole and heavy-hole transitions are merged together. Now the probe is on the left-hand side of the absorption feature and hence is about π out of phase with the 8-T signal [cf. Fig. 3(c)].

Finally, we present the comparison of the experiment and theory when it comes to the *period* of the CP's oscillations in Fig. 9. Shown is the experimentally measured period of the CP's oscillations at the initial propagation times <40 ps (red star) and longer times >50 ps (violet circle) as a function of magnetic field. The red dashed line is a theoretical calculation based on the formula in an earlier study by Blakemore [49] using $n = 3.65$ and $v_{LA} = 4.73$ nm/ps. The blue line is an estimate for the $Ga_{1-x}Mn_xAs$, with $x = 0.07$ at 78 K from Fig. 4 in Qi *et al.* [4]. For low magnetic fields, $B < 2$ T, we see that the GaMnAs can contribute to the signal during the short time that the pulse from the interface is in the GaMnAs film. For large fields, $B > 3$ T for the same time window is dominated by the GaAs response. This is consistent with Fig. 6(c), which shows that the enhancement factor contribution from the GaAs and GaMnAs layers are comparable at low fields, but at high fields, the GaAs enhancement factor is much stronger.

[1] S. Kobayashi, Y. Hashimoto, and H. Munekata, J. Appl. Phys. **105**, 07C519 (2009).
[2] J. Wang, G. A. Khodaparast, J. Kono, A. Oiwa, and H. Munekata, J. Mod. Opt. **51**, 2771 (2004).
[3] J. Wang, C. Sun, Y. Hashimoto, J. Kono, G. A. Khodaparast, L. Cywinski, L. J. Sham, G. D. Sanders, C. J. Stanton, and H. Munekata, J. Phys.: Condens. Matter **18**, R501 (2006).
[4] J. Qi, J. A. Yan, H. Park, A. Steigerwald, Y. Xu, S. N. Gilbert, X. Liu, J. K. Furdyna, S. T. Pantelides, and N. Tolk, Phys. Rev. B **81**, 115208 (2010).
[5] A. V. Kimel, G. V. Astakhov, G. M. Schott, A. Kirilyuk, D. R. Yakovlev, G. Karczewski, W. Ossau, G. Schmidt, L. W. Molenkamp, and T. Rasing, Phys. Rev. Lett. **92**, 237203 (2004).
[6] Y. Hashimoto, S. Kobayashi, and H. Munekata, Phys. Rev. Lett. **100**, 067202 (2008).
[7] M. Dobrowolska, K. Tivakornsasithorn, X. Liu, J. Furdyna, M. Berciu, K. Yu, and W. Walukiewicz, Nat. Mater. **11**, 444 (2012).
[8] C. P. Weber, E. A. Kittlaus, K. B. Mattia, C. J. Waight, J. Hagmann, X. Liu, M. Dobrowolska, and J. K. Furdyna, Appl. Phys. Lett. **102**, 182402 (2013).
[9] H. Jeong, Y. D. Jho, and C. J. Stanton, Phys. Rev. Lett. **114**, 043603 (2015).
[10] H. Jeong, Y. D. Jho, S. H. Rhim, K. J. Yee, S. Y. Yoon, J. P. Shim, D. S. Lee, J. W. Ju, J. H. Baek, and C. J. Stanton, Phys. Rev. B **94**, 024307 (2016).
[11] C. Thomseen, H. T. Grahn, H. J. Maris, and J. Tauc, Opt. Commun. **60**, 55 (1986).
[12] J.-K. Yu, S. Mitrovic, D. Tham, J. Varghese, and J. R. Heath, Nat. Nanotechnol. **5**, 718 (2010).
[13] G. Pernot, M. Stoffel, I. Savic, F. Pezzoli, P. Chen, G. Savelli, A. Jacquot, J. Schumann, U. Denker, I. Monch, Ch. Deneke, O. G. Schmidt, J. M. Rampnoux, S. Wang, M. Plissonnier, A. Rastelli, S. Dilhaire, and N. Mindo, Nat. Mater. **9**, 491 (2010).
[14] E. S. K. Young, A. V. Akimov, M. Henini, L. Eaves, and A. J. Kent, Phys. Rev. Lett. **108**, 226601 (2012).
[15] I. S. Grudinin, H. Lee, O. Painter, and K. J. Vahala, Phys. Rev. Lett. **104**, 083901 (2010).
[16] R. P. Beardsley, A. V. Akimov, M. Henini, and A. J. Kent, Phys. Rev. Lett. **104**, 085501 (2010).
[17] A. Fainstein, N. D. Lanzillotti-Kimura, B. Jusserand, and B. Perrin, Phys. Rev. Lett. **110**, 037403 (2013).
[18] I. Mahboob, K. Nishiguchi, A. Fujiwara, and H. Yamaguchi, Phys. Rev. Lett. **110**, 127202 (2013).
[19] S. J. Whiteley, G. Wolfowicz, C. P. Anderson, A. Bourassa, H. Ma, M. Ye, G. Koolstra, K. J. Satzinger, M. V. Holt, F. J. Heremans *et al.*, Nat. Phys. **15**, 490 (2019).
[20] C. Thomsen, H. T. Grahn, H. J. Maris, and J. Tauc, Phys. Rev. B **34**, 4129 (1986).
[21] A. V. Kuznetsov and C. J. Stanton, Phys. Rev. Lett. **73**, 3243 (1994).

[22] L. Thevenard, E. Peronne, C. Gourdon, C. Testelin, M. Cubukcu, E. Charron, S. Vincent, A. Lemaître, and B. Perrin, Phys. Rev. B **82**, 104422 (2010).
[23] A. N. Poddubny, A. V. Poshakinskiy, B. Jusserand, and A. Lemaître, Phys. Rev. B **89**, 235313 (2014).
[24] O. B. Wright, B. Perrin, O. Matsuda, and V. E. Gusev, Phys. Rev. B **64**, 081202(R) (2001).
[25] N. Miura, Compr. Semicond. Sci. Technol. **2**, 256 (2011).
[26] T. Matsuda and H. Munekata, Phys. Rev. B **93**, 075202 (2016).
[27] A. Pogrebna, S. Barsaume, R. R. Subkhangulov, A. V. Telegin, Y. P. Sukhorukov, A. V. Chzhan, T. Rasing, and A. V. Kimel, Phys. Rev. B **98**, 214427 (2018).
[28] M. Raskin, T. Stiehm, A. W. Cohn, K. M. Whitaker, S. T. Ochsenbein, S. M. de Vasconcellos, M. S. Brandt, D. R. Gamelin, and R. Bratschitsch, Phys. Status Solidi B **251**, 1685 (2014).
[29] V. N. Kats, T. L. Linnik, A. S. Salasyuk, A. W. Rushforth, M. Wang, P. Wadley, A. V. Akimov, S. A. Cavill, V. Holy, A. M. Kalashnikova *et al.*, Phys. Rev. B **93**, 214422 (2016).
[30] E. Beaurepaire, J.-C. Merle, A. Daunois, and J.-Y. Bigot, Phys. Rev. Lett. **76**, 4250 (1996).
[31] J. Wang, C. Sun, J. Kono, A. Oiwa, H. Munekata, L. Cywiński, and L. J. Sham, Phys. Rev. Lett. **95**, 167401 (2005).
[32] B. Koopmans, G. Malinowski, F. Dalla Longa, D. Steiauf, M. Fähnle, T. Roth, M. Cinchetti, and M. Aeschlimann, Nat. Mater. **9**, 259 (2010).
[33] J. V. Jäger, A. V. Scherbakov, B. A. Glavin, A. S. Salasyuk, R. P. Campion, A. W. Rushforth, D. R. Yakovlev, A. V. Akimov, and M. Bayer, Phys. Rev. B **92**, 020404(R) (2015).
[34] J. Wang, Y. Hashimoto, J. Kono, A. Oiwa, H. Munekata, G. D. Sanders, and C. J. Stanton, Phys. Rev. B **72**, 153311 (2005).
[35] K. J. Yee, Y. S. Lim, X. Liu, W. L. Lim, D. S. Kim, and M. Dobrowolska, J. Supercond. **18**, 115 (2005).
[36] J. P. Zahn, A. Gamouras, S. March, X. Liu, J. K. Furdyna, and K. C. Hall, J. Appl. Phys. **107**, 033908 (2010).
[37] S. Lee, J.-H. Chung, X. Liu, J. K. Furdyna, and B. J. Kirby, Mater. Today **12**, 14 (2009).
[38] R. R. H. H. Mudiyanselage, B. A. Magill, J. Burton, M. Miller, J. Spencer, K. McMillan, G. A. Khodaparast, H. B. Kang, M. G. Kang, D. Maurya *et al.*, J. Mater. Chem. C **7**, 14212 (2019).
[39] O. Matsuda, O. B.Wright, D. H. Hurley, V. E. Gusev, and K. Shimizu, Phys. Rev. Lett. **93**, 095501 (2004).
[40] C. Cook, S. Khan, G. Sanders, X. Wang, D. Reitze, Y. Jho, Y.-W. Heo, J.-M. Erie, D. Norton, and C. Stanton, in *Oxide-Based Materials and Devices* (International Society for Optics and Photonics, Bellingham, WA, 2010), Vol. 7603, p. 760304.
[41] A. Baydin, R. Gatamov, H. Krzyzanowska, C. J. Stanton, and N. Tolk, Phys. Rev. B **99**, 165202 (2019).
[42] G. D. Sanders, C. J. Stanton, J. Wang, J. Kono, A. Oiwa, and H. Munekata, Phys. Rev. B **72**, 245302 (2005).
[43] P. Y. Yu and M. Cardona, *Fundamentals of Semiconductors, Physics and Material Properties* (Springer, Berlin, 1995).
[44] M. A. Meeker, B. A. Magill, G. A. Khodaparast, D. Saha, C. J. Stanton, S. McGill, and B. W. Wessels, Phys. Rev. B **92**, 125203 (2015).
[45] Y. Sun, F. V. Kyrychenko, C. J. Stanton, G. A. Khodaparast, J. Kono, Y. H. Matsuda, and H. Munekata, Spin **5**, 1550002 (2015).
[46] The initial oscillation for the first 45 ps results from half of the strain pulse generated at the interface traveling to the right into the GaAs substrate. As discussed previously, the strain pulse in the GaMnAs only very weakly affects the signal.
[47] A. K. Basak, H. Petek, K. Ishioka, E. M. Thatcher, and C. J. Stanton, Phys. Rev. B **91**, 125201 (2015).
[48] K. L. Pollock, H. Q. Doan, A. Rustagi, C. J. Stanton, and T. Cuk, J. Phys. Chem. Lett. **8**, 922 (2017).
[49] J. S. Blakemore, J. Appl. Phys. **53**, R123 (1982).